

# UCLA

## UCLA Previously Published Works

### Title

The Stringent Response Contributes to Persistent Methicillin-Resistant *Staphylococcus aureus* Endovascular Infection Through the Purine Biosynthetic Pathway.

### Permalink

<https://escholarship.org/uc/item/2bd0g9pm>

### Journal

The Journal of Infectious Diseases, 222(7)

### ISSN

0022-1899

### Authors

Li, Liang  
Bayer, Arnold S  
Cheung, Ambrose  
[et al.](#)

### Publication Date

2020-09-01

### DOI

10.1093/infdis/jiaa202

Peer reviewed

# The Stringent Response Contributes to Persistent Methicillin-Resistant *Staphylococcus aureus* Endovascular Infection Through the Purine Biosynthetic Pathway

Liang Li,<sup>1</sup> Arnold S. Bayer,<sup>1,2,3</sup> Ambrose Cheung,<sup>4</sup> Lou Lu,<sup>1,2,5</sup> Wessam Abdelhady,<sup>1</sup> Niles P. Donegan,<sup>4</sup> Jong-In Hong,<sup>6</sup> Michael R. Yeaman,<sup>1,2,3,5</sup> and Yan Q. Xiong<sup>1,2,3</sup>

<sup>1</sup>Lundquist Institute for Biomedical Innovation at Harbor-UCLA Medical Center, Torrance, California, USA, <sup>2</sup>Division of Infectious Diseases, Department of Medicine, Harbor-UCLA Medical Center, Torrance, California, USA, <sup>3</sup>David Geffen School of Medicine at UCLA, Los Angeles, California, USA, <sup>4</sup>Geisel School of Medicine at Dartmouth, Hanover, New Hampshire, USA, <sup>5</sup>Division of Molecular Medicine, Department of Medicine, Harbor-UCLA Medical Center, Torrance, California, USA, and <sup>6</sup>Department of Chemistry, Seoul National University, Seoul, Korea

Persistent methicillin-resistant *Staphylococcus aureus* (MRSA) endovascular infections represent a significant clinical-therapeutic challenge. Of particular concern is antibiotic treatment failure in infections caused by MRSA that are “susceptible” to antibiotic in vitro. In the current study, we investigate specific purine biosynthetic pathways and stringent response mechanism(s) related to this life-threatening syndrome using genetic matched persistent and resolving MRSA clinical bacteremia isolates (PB and RB, respectively), and isogenic MRSA strain sets. We demonstrate that PB isolates (vs RB isolates) have significantly higher (p)ppGpp production, phenol-soluble-modulin expression, polymorphonuclear leukocyte lysis and survival, fibronectin/endothelial cell (EC) adherence, and EC damage. Importantly, an isogenic strain set, including JE2 parental, *relP*-mutant and *relP*-complemented strains, translated the above findings into significant outcome differences in an experimental endocarditis model. These observations indicate a significant regulation of purine biosynthesis on stringent response, and suggest the existence of a previously unknown adaptive genetic mechanism in persistent MRSA infection.

**Keywords.** MRSA; stringent response; (p)ppGpp; purine biosynthesis; persistence; endovascular infection.

Infective endocarditis (IE) is a life-threatening syndrome often caused by methicillin-resistant *Staphylococcus aureus* (MRSA) [1]. Despite the use of gold-standard anti-MRSA antibiotics, (vancomycin [VAN] or daptomycin [DAP]), treatment failures associated with these syndromes remain unacceptably high (~ 30%) [2, 3]. Persistent MRSA bacteremia (PB; defined as ≥ 7 days of positive blood cultures despite appropriate antibiotic therapy) occurs in 15%–30% of such infections. This phenomenon is very worrisome because many PB strains are typically “susceptible” in vitro to standard-of-care anti-MRSA agents such as VAN and DAP as determined by Clinical and Laboratory Standards Institute breakpoints [3, 4]. Therefore, PB outcomes pose an urgent and unmet therapeutic challenge to public health. Understanding the specific molecular mechanisms of PB is essential to develop novel anti-MRSA strategies to prevent or minimize the persistent outcomes.

The stringent response is a highly conserved adaptation mechanism to stressful conditions (eg, antibiotic pressure),

initiated by the rapid synthesis of a bacterial alarmone, guanosine 3′-diphosphate-5′-di(tri)phosphate [(p)ppGpp] [5–8]. *Staphylococcus aureus* possesses 3 (p)ppGpp synthetases: the bifunctional Rel<sub>Sau</sub> protein, with hydrolase and synthetase functions, and 2 small alarmone synthetases, RelP (RelP<sub>Sau</sub>) and RelQ (RelQ<sub>Sau</sub>) [9, 10] (Figure 1). While the stringent response has been well studied in other organisms, particularly in gram-negative bacteria [5, 11], neither its impact on the PB outcomes nor its intersection with purine biosynthesis has been evaluated in MRSA endovascular infections.

De novo purine biosynthesis represents a basis for nucleotide metabolism and is critical for bacterial cell growth through nucleobase syntheses (eg, GDP and GTP) [12]. (p)ppGpp is synthesized from GDP/GTP [10, 13] and could also provide feedback control of GTP levels by inhibiting GTP biosynthesis enzymes [14, 15]. We recently demonstrated a critical role of purine biosynthesis in the PB outcomes [16]. Those studies led us to hypothesize that the purine biosynthesis impact on GDP/GTP affects (p)ppGpp synthesis, which in turn provides a link to the stringent response in adaptive survival mechanisms of MRSA (Figure 1). The current investigation was designed to test these hypotheses by studying the interrelationships among purine biosynthesis, the stringent response, and PB vs resolving MRSA clinical bacteremia (RB, defined as initial bacteremia resolved within 2–4 days to therapy) outcomes both in vitro and in an experimental IE model.

Received 16 January 2020; editorial decision 15 April 2020; accepted 21 April 2020; published online April 25, 2020.

Correspondence: Y. Q. Xiong, MD, PhD, Lundquist Institute for Biomedical Innovation at Harbor-UCLA Medical Center, 1124 W Carson St, Torrance, CA 90502 (yxiong@ucla.edu).

The Journal of Infectious Diseases® 2020;222:1188–98

© The Author(s) 2020. Published by Oxford University Press for the Infectious Diseases Society of America. All rights reserved. For permissions, e-mail: journals.permissions@oup.com. DOI: 10.1093/infdis/jiaa202

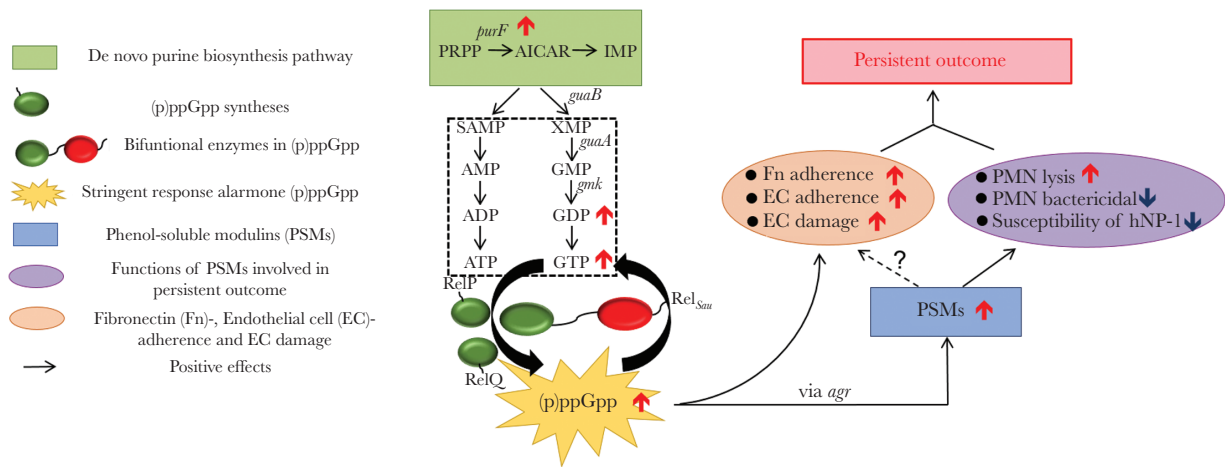


**Figure 1.** Hypothesized model of the role of purine biosynthesis and the stringent response alarmone, (p)ppGpp, in persistent methicillin-resistant *Staphylococcus aureus* (MRSA) endovascular infection. De novo purine biosynthesis pathway mediates the conversion of 5-phosphoribosyl-1-pyrophosphate (PRPP) to inosine monophosphate (IMP), which subsequently become purines ATP and GTP. The stringent response alarmone, guanosine 3'-diphosphate-5'-di(tri)phosphate [(p)ppGpp], is mainly produced from GDP/GTP, and its production is controlled by a bifunctional synthetase *Rel<sub>Sau</sub>* protein, and 2 other monofunctional synthetases *RelP* and *RelQ* in *S. aureus* [5–10]. The elevated expression of *purF* gene, encoding a rate-limited enzyme ATPase (PRPP→PRA), in the purine biosynthesis pathway leads to increased GDP/GTP and subsequent (p)ppGpp levels. Increased (p)ppGpp leads to up-regulation (*agr*-dependent) of persistent-related factors, such as (1) phenol-soluble modulins (PSMs), which increase *S. aureus*-induced Neutrophils (PMN) lysis and support *S. aureus* to overcome PMN- and human neutrophil peptide 1 (hNP-1)-mediated bactericidal killing; and (2) MRSA-endothelial cell (EC) interactions, including enhanced fibronectin (Fn)/EC adherence and EC damage, and eventually facilitating persistent MRSA bacteremia outcomes.

## METHODS

### Bacterial Strain and Plasmids

Bacterial strains and plasmids used in the current study are listed in Table 1. Eight representative clinical MRSA isolates (1

PB and 1 RB strain for each of the 4 most common clonal complex [CC] and *agr* types) were obtained from a multinational clinical trial collection and other sources [4, 17]. All of the MRSA isolates were VAN-susceptible (MICs ≤ 2 µg/mL) and

**Table 1. Bacterial Strains and Plasmids Used in This Study**

Strains and Plasmids	Description	Vancomycin MIC, µg/mL	References
<b>Clinical MRSA isolates</b>			
PB: 300-169	<i>agr-I</i> , <i>SCCmec IV</i> , CC45, fast-growth rate <sup>a</sup> , early global regulators onset <sup>b</sup> , nonresponder <sup>c</sup>	0.5	[4, 16]
RB: 301-188	<i>agr-I</i> , <i>SCCmec IV</i> , CC45, slow-growth rate, late global regulators onset, responder <sup>d</sup>	0.5	[4, 16]
PB: 300-246	<i>agr-II</i> , <i>SCCmec I</i> , CC5, fast-growth rate, early global regulators onset, nonresponder	0.5	[4, 16]
RB: 010-016	<i>agr-II</i> , <i>SCCmec II</i> , CC5, slow-growth rate, late global regulators onset, responder	0.5	[4, 16]
PB: 31082	<i>agr-I</i> , <i>SCCmec IV</i> , CC8, fast-growth rate, early global regulators onset, nonresponder	2.0	[16, 18]
RB: 30568	<i>agr-I</i> , <i>SCCmec IV</i> , CC8, slow-growth rate, late global regulators onset, responder	2.0	[16, 18]
PB: 33367	<i>agr-III</i> , <i>SCCmec II</i> , CC30, fast-growth rate, early global regulators onset, nonresponder	1.0	[16, 18]
RB: 22033	<i>agr-III</i> , <i>SCCmec II</i> , CC30, slow-growth rate, late global regulators onset, responder	1.0	[16, 18]
LAC*	Erm sensitive community-acquired MRSA LAC strain (USA300)	...	[23]
<b>Laboratory MRSA strains</b>			
JE2	LAC, USA300 derivative that was cured of its 3 plasmids ( <i>agr-I</i> , <i>SCCmec IV</i> , CC8)	2.0	[19]
LAC* <i>rsh<sub>syn</sub></i>	LAC variant that lacked 3 conserved amino acids in the (p)ppGpp synthetase domain of <i>Rel<sub>Sau</sub></i>	...	[23]
JE2 $\Delta$ <i>relP</i>	Transposon mutant with insertion in USA300_2446	2.0	NTML
JE2 $\Delta$ <i>purF</i>	Transposon mutant with insertion in USA300_0972	2.0	NTML
JE2 $\Delta$ <i>relP</i> / <i>prelP</i>	JE2 $\Delta$ <i>relP</i> complemented with plasmid pSK236:: <i>relP</i>	2.0	This study
JE2 $\Delta$ <i>purF</i> / <i>ppurF</i>	JE2 $\Delta$ <i>purF</i> complemented with plasmid pSK236:: <i>purF</i>	2.0	[16]

Abbreviations: CC, clonal complex; MIC, minimum inhibitory concentration; MRSA, methicillin-resistant *Staphylococcus aureus*; NTML, Nebraska Transposon Mutant Library; PB, persistent methicillin-resistant *Staphylococcus aureus* bacteremia; RB, resolving methicillin-resistant *Staphylococcus aureus* bacteremia.

<sup>a</sup>TSB medium, aerobic, 37°C [16].

<sup>b</sup>Global regulators: *sigB*, *sarA*, *sae*, *agr-RNAIII* [4, 16].

<sup>c</sup>Nonresponder, the isolates in which < 1.5-log<sub>10</sub> colony-forming units (CFU) mean reductions per gram of vegetation, kidney, and spleen were observed due to vancomycin treatment in a rabbit infective endocarditis (IE) model [4].

<sup>d</sup>Responder, the isolates in which vancomycin treatment caused a ≥ 5-log<sub>10</sub> CFU mean reduction per gram of vegetation and ≥ 3-log<sub>10</sub> CFU mean reduction/g of kidney or spleen in IE model [4].

had neither VAN in vitro tolerance nor VAN heteroresistant subpopulations [4, 17, 18]. JE2 (USA300 LAC derivative cured of 3 plasmids [19]) and its isogenic *purF* and *relP* mutant strains from Nebraska transposon mutant library were also used in this study. The *relP* mutant was complemented by transforming plasmid pSK236::*relP* as described previously [20].

#### Determination of VAN MICs

MICs of VAN were determined by a standard Etest method (bioMérieux, LABalme-les-Grottes, France).

#### Detection of (p)ppGpp Levels

The intracellular (p)ppGpp levels of the study MRSA strains were detected by using a fluorescent chemosensor, PyDPA, as previously described [21, 22]. In brief, exponential phase (3 hours' incubation) MRSA cells were harvested and adjusted at optical density (wavelength at 600 nm; OD<sub>600nm</sub>) of 1.000. This time point was used based on our previous studies showing earlier-onset activation (2–4 hours' incubation) of key global regulators in the PB vs RB strains [16, 17]. After adding lysis reagent (100% methanol), the supernatant was collected and concentrated by using a lyophilizer. The dried extracts were then suspended in HEPES buffer (1 mM, pH 7.4 containing 16% dimethyl sulfoxide [v/v]), and mixed with PyDPA (40 μM) [21, 22]. Fluorescence was measured using a Perkin-Elmer LS-55 fluorescence spectrometer with Ex 344 nm/Em 470 nm for (p)ppGpp levels [21, 22]. The samples extracted from LAC<sup>+</sup> strain treated with mupirocin and LAC<sup>+</sup>*rsh*<sub>syn</sub> strain were used as positive and negative controls, respectively [23].

#### Detection of GDP and GTP Levels

The intracellular GDP levels of the study MRSA cells from exponential phase growth (3 hours' incubation) were detected by using a Transcreener GDP FI kit (BellBrook Labs) [24]. GDP levels were expressed as fluorescence intensity. GTP levels were quantified by a luciferase-based assay using Promega BacTiter Glo and GTPase-Glo Kinase Kits (Promega) [25–27]. In brief, samples from the (p)ppGpp detection assay were mixed with an equal volume of GTPase-Glo reagent to convert GTP to ATP. After 30 minutes of incubation at room temperature, total ATP including the residual ATP and that generated in this reaction was detected using a luciferin/luciferase-based ATP detection reagent. In parallel, the residual ATP levels in extracted samples were measured, samples from the (p)ppGpp detection assay were mixed with an equal volume of BacTiter-Glo reagent and incubated for 5 minutes at room temperature, and ATP levels were determined by measuring luminescence levels. GTP levels (luminescence intensity) were presented as the total luminescence levels minus residual ATP luminescence levels [25, 27].

#### RNA Isolation and Target Gene Expression by Reverse-Transcription-Quantitative Polymerase Chain Reaction

Total RNA of the study MRSA strains from the exponential phase (3 hours' incubation) was isolated by using a RNeasy Kit

(Qiagen) [28]. One microgram of DNase-treated RNA was transcribed into complementary DNA. Real-time quantitative polymerase chain reaction (qPCR) was performed using a SYBR green PCR master kit (Applied Biosystems). The amplification of *psma1–4*, *psmβ1,2* and *gyrB* was performed using primers as described previously [4, 29]. *gyrB* was used to normalize the transcript quantification. The relative quantification of gene expression was calculated by the  $\Delta\Delta C_T$  method [4].

#### Neutrophils (PMN) Bactericidal Activity and MRSA-Induced PMN Lysis

Human neutrophil-mediated killing was performed as described previously [29, 30]. In brief, exponential phase MRSA cells were washed and adjusted to OD<sub>600nm</sub> of 1.000 in Hanks' balanced salt solution (HBSS). Frozen human neutrophils obtained from Astarte Biologics were thawed in 37°C water bath and gently resuspended in HBSS [31]. The bacterial suspension was mixed to 10<sup>6</sup> colony-forming units (CFU)/mL neutrophils with the initial ratios 10:1 (bacteria:neutrophils). The percentage of bacterial survival was expressed as the percentage of the initial inoculum that survived with neutrophils exposure. Following the PMN bactericidal activity experiment above, lysis of the human neutrophils was determined with a standard release of lactate dehydrogenase assay according to the manufacturer's recommended protocols (Cytotoxicity Detection kit, Roche Applied Sciences) [29, 32].

#### In Vitro Susceptibility to Human Neutrophil Peptide 1

The human neutrophil peptide 1 (hNP-1) susceptibility was detected by exposing 10<sup>5</sup> CFU/mL MRSA cells from exponential phase growth to hNP-1 (Peptides International) at 1.25 μg/mL according to the method described previously [33, 34]. Survival rates were expressed as the survival cells compared to the initial inoculum.

#### In Vitro Susceptibility to VAN

A starting inoculum of 10<sup>8</sup> CFU/mL of MRSA cells at exponential phase were exposed to 15 μg/mL of VAN (mimic targeted trough serum level of VAN treatment for severe MRSA infections in human) in cation-adjusted MHB for 24 hours [4, 18]. Survival rates were expressed as the survival cells compared to the initial inoculum.

#### Adherence to Fibronectin

A starting inoculum of 5 × 10<sup>3</sup> CFU/well of exponential phase MRSA cells were added to the 6-well plates coated with purified human fibronectin (Fn) (50 μg/mL, Sigma Chemicals) and incubated for 1 hour at 37°C. The adherence was expressed as the percentage of the initial inoculum bound [35].

#### Endothelial Cell Adherence

Human microvascular endothelial cells (HMEC-1) were obtained from the Centers for Disease Control and Prevention and maintained as previously described [36, 37]. MRSA exponential phase cells were added to plate confluent with HMEC-1

cells at a final inoculum of  $5 \times 10^3$  CFU/well and incubated for 1 hour at 37°C [38]. The adherence rate was expressed as a percentage of the initial inoculum [38].

#### Endothelial Cell Damage

A well-established 3-(4,5-dimethylthiazol-2-yl)-2,5-diphenyltetrazolium bromide (MTT) assay was used to test the endothelial cell (EC) damage [39]. In brief, exponential phase MRSA cells were added to HMEC-1 in 24-well plates ( $5 \times 10^5$  ECs/well) corresponding to a multiplicity of infection of 50 (as established by pilot studies). After 3 hours of incubation, the wells were washed with HBSS and medium containing lysostaphin (10 µg/mL, Sigma Chemicals) was added to lyse extracellular MRSA cells [39]. After 18 hours of incubation, 100 µL of MTT (5 mg/mL, Sigma Chemicals) was added and incubated for 2 hours. The medium was replaced with 150 µL of 0.04 M HCl to stop the reaction. Absorbance was measured at OD<sub>560nm</sub>. HMEC-1 without MRSA exposure was considered 0% damage control. The damage was presented as a percentage of  $1 - (\text{OD}_{560\text{nm}}$  values of samples / OD<sub>560nm</sub> values of control) [39].

#### Experimental IE Model in Rabbits

A well-characterized rabbit model of catheter-induced aortic valve endocarditis was used to validate the in vivo role of stringent response in persistent MRSA outcomes [33, 40]. The Institutional Animal Care and Use Committee of the Lundquist Institute for Biomedical Innovation at Harbor–University of California, Los Angeles Medical Center approved all animal study protocols. After 72 hours of catheterization, animals were infected intravenously of JE2 parental, its isogenic *relP* mutant or *relP*-complemented strain at  $10^5$  CFU/animal, an 95% infective dose (ID<sub>95</sub>) as established previously [28, 40]. At 24 hours postinfection, animals were randomized to receive no therapy (controls) or VAN (3.75 mg/kg, intravenously, twice daily for 3 days). VAN-treated animals were sacrificed at 24 hours after the last treatment dose to avoid VAN carryover effect. At sacrifice, cardiac vegetation, kidney, and spleen were sterilely removed and quantitatively cultured [28, 40]. MRSA counts in the target tissues were given as the mean log<sub>10</sub> CFU/g of tissue ( $\pm$  standard deviation).

#### Statistical Analysis

All in vitro experiments were performed in triplicate and repeated 3 times. Statistical significance values were obtained by performing 2-tailed Student *t* test, or 1-way analysis of variance with Tukey multiple comparisons test (no adjustment). *P* values of  $< .05$  were considered statistically significant.

## RESULTS

#### PB Strains Exhibit Significantly Higher (p)ppGpp, GDP, and GTP Levels Than RB Strains

(p)ppGpp levels were tested by using a fluorescent chemosensor PyDPA method [21, 22]. We first validated this

assay by demonstrating significant lesser and greater fluorescence intensities representing (p)ppGpp levels in the negative (LAC\**rsh*<sub>syn</sub> mutant strain) and positive (LAC\* + mupirocin) controls vs LAC\* parental strain, respectively (Figure 2A;  $P < .0001$ ). Significantly higher (p)ppGpp levels were observed in PB strains vs their respective matched RB strains (Figure 2B;  $P < .05$ ). We hypothesized that higher levels of (p)ppGpp would plausibly be due to elevated GDP/GTP levels in PB vs RB isolates. Indeed, significantly higher intracellular GDP and GTP levels were observed in PB strains vs their respective RB strains (Figure 2C and 2D).

#### PB Strains Express Higher *psm* Levels Than RB Strains

The stringent response from (p)ppGpp can regulate the production of phenol-soluble modulins (PSMs), which have been shown to play key roles in lysis of PMN [29, 41], thus contributing to the disruption of the host innate immune defense. We demonstrated that PB isolates exhibited significantly higher expression of *psma1-4* (1.4- to 1.9-fold;  $P < .0001$ ), the more active form of PSM, relative to their respective matched RB comparators (Figure 3A). Additionally, 3 of the 4 PB isolates showed substantial higher *psmβ1-2* expression (2.1- to 2.8-fold) vs their respective RB counterparts (Figure 3A;  $P < .0001$ ).

#### PSMs Correspond to Phenotypes Related to PB Outcomes

PSMs have been shown to mediate PMN lysis and dysfunction to promote *S. aureus* survival [41]. We noted that PB strains caused significantly greater PMN lysis (range, 18.4%–33.6%) than their respective matched RB strains (range, 10.4%–22.3%; Figure 3B), paralleling the increased *S. aureus* survival in PMN killing assay (51%–71% and 37%–44% in PB and RB strains, respectively; Figure 3B). As defensin contributes to the bactericidal activity within the phagolysosomes of PMNs, we also evaluated the sensitivity of PB vs RB isolates. As shown in Figure 3C, PB strains had significantly higher survival upon exposure to hNP-1 as compared to their respective RB strains.

#### Isogenic *purF* Mutants Validate the Causal Relationship Among Adaptive Purine Biosynthesis Regulation, Stringent Response, and PB Phenotypes

To verify that the above findings are linked to purine synthesis, MRSA parental strain JE2, its isogenic *purF*-mutant and *purF*-complemented strains were examined. Consistently, the *purF* mutant (a surrogate for RB clinical strains [16]) had significantly decreased (p)ppGpp, GDP, and GTP levels (Figure 4A;  $P < .05$ ) vs its isogenic parental and *purF*-complemented strains. In addition, the *purF* mutant exhibited significantly reduced *psma1-4* and *psmβ1,2* transcription (Figure 4B;  $P < .01$ ), in association with lower PMN lysis and survival vs its isogenic parental and *purF*-complemented strains (Figure 4C;  $P < .05$ ). Also, greater hNP-1-induced killing was observed in the *purF* mutant (survival rate, 27.5%) vs its isogenic parental and *purF*-complemented strains (survival rate, 49.2% and 44.0%,



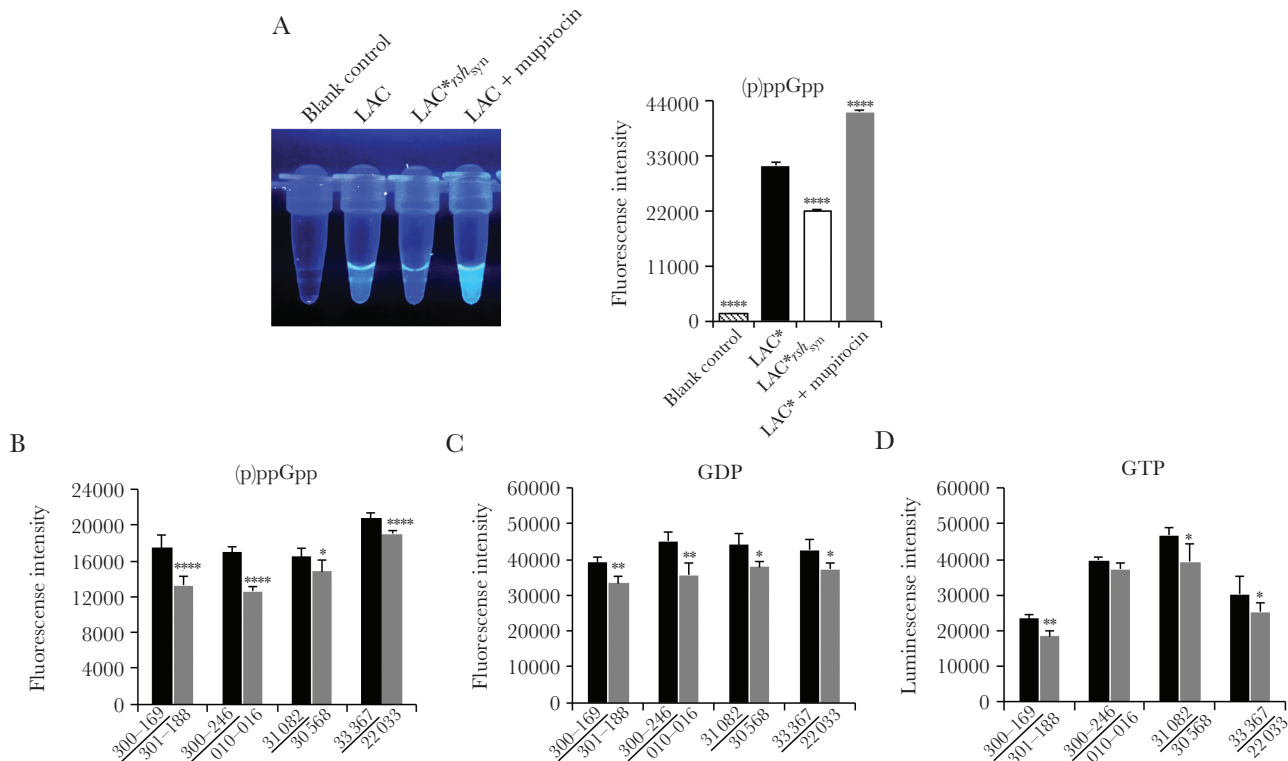


**Figure 2.** Increased (p)ppGpp associated with higher GDP and GTP levels in clinical persistent methicillin-resistant *Staphylococcus aureus* (MRSA) bacteremia (PB; underlined) vs resolving MRSA bacteremia (RB) strains. A, (p)ppGpp levels (fluorescence intensity) in buffer alone (blank control), LAC\*, LAC\**rsh<sub>syn</sub>* (negative control), and mupirocin-treated LAC\* (positive control). Levels of (p)ppGpp (B), GDP (C), and GTP (D) in PB vs RB clinical strains. Data are representative of 3 independent experiments. \* $P < .05$ , \*\* $P < .01$ , \*\*\* $P < .001$ , \*\*\*\* $P < .0001$  vs the parental strain LAC\* or their respective matched PB strain by Student *t* test. Error bars represent standard deviations.

respectively;  $P < .05$ ). To establish persistence, *S. aureus* must adhere to matrix ligands (eg, Fn) on host cells such as ECs, and damage host cells to facilitate disease and dissemination [38, 42]. We demonstrated that the *purF* mutant had significantly less Fn/EC adherence, and reduced EC damage vs its isogenic parental and *purF*-complemented strains (Figure 4D;  $P < .01$ ).

#### (p)ppGpp Positively Impacts Coordinated Virulence Phenotypes Involved in Persistence

To assess the role of (p)ppGpp in the regulation of PSMs and its impacts on the phenotypes related to the PB outcomes, the parental strain JE2, its isogenic *relP* mutant, and *relP*-complemented strain set was used (Table 1). A significantly lower (p)ppGpp level was demonstrated in the *relP* mutant vs its parental strain and restored in the *relP*-complemented strain (Figure 5A;  $P < .0001$ ). Importantly, akin to the RB clinical isolates and the *purF* mutant strain, the *relP* mutant of JE2 exhibited multiple phenotypes associated with RB: (1) significantly decreased *psmA1-4* and *psmβ1,2* expression (Figure 5B); (2) reduced PMN lysis and less survival in PMNs exposure (Figure 5C;  $P < .05$ ); (3) decreased at least 0.5-fold survival rates against hNP-1 and VAN ( $P < .01$ ); and (4) less Fn/EC adherence accompanied by reduced EC damage (Figure 5D;  $P < .01$ ) vs its isogenic JE2 parental and *relP*-complemented strains.

#### Stringent Response Alters the Efficacy of VAN in an Experimental IE Model

To affirm the impact of the stringent response in a relevant *in vivo* context, the role of the *relP*-mediated stringent response relative to PB outcome was investigated in a rabbit IE model. Results demonstrated that rabbits infected with the JE2 parent, *relP* mutant, or *relP*-complemented strain had equivalent virulence in the absence of VAN treatment, reflected in similar MRSA densities in key target tissues (Figure 6). Upon VAN treatment, rabbits infected with the *relP* mutant strain became hypersusceptible, with significantly reduced MRSA densities in all target tissues as compared to the parent and *relP*-complemented strains (Figure 6).

#### DISCUSSION

The stringent response is a highly conserved adaptive survival mechanism in bacteria that is activated in response to various environmental stresses [10, 22]. We recently demonstrated that enhanced purine biosynthesis triggers a faster growth phenotype in PB vs RB strains [16]. Kriel et al observed that elevated GTP levels might result in increased ppGpp levels in *Bacillus subtilis* [14]. We thus postulated that augmented purine biosynthesis with enhanced growth generates key intermediates (eg, GDP and GTP) that are critical to the synthesis of (p)ppGpp

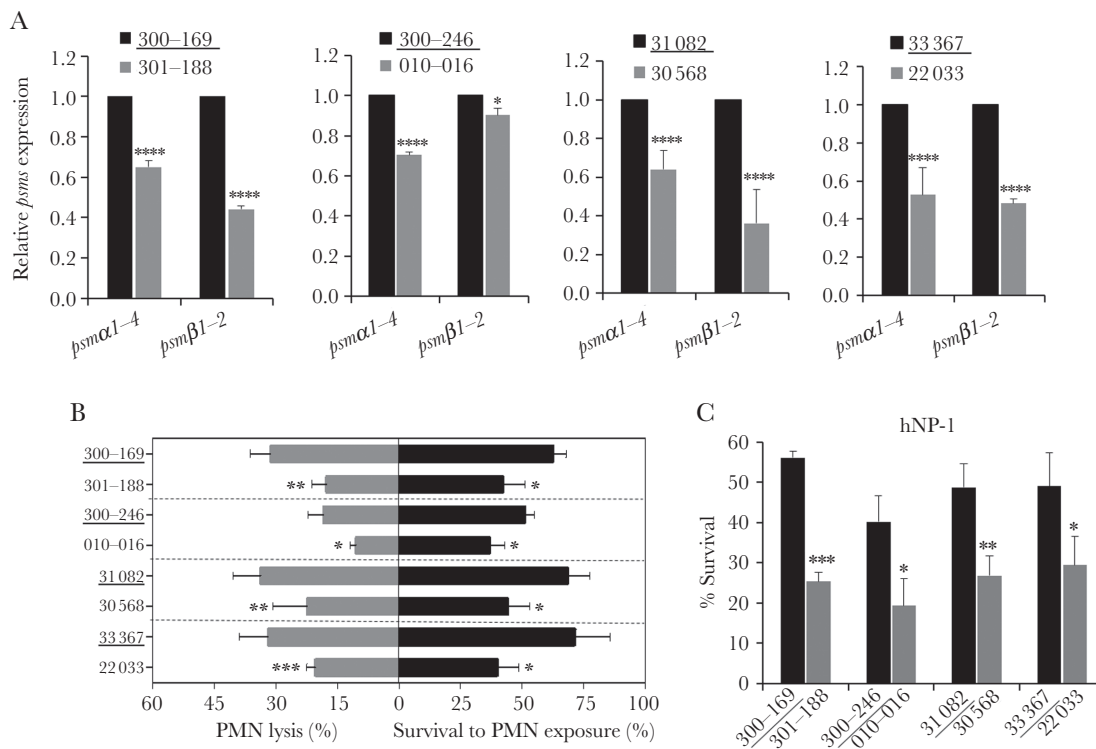


**Figure 3.** *psms* expression and its impacts on persistent methicillin-resistant *Staphylococcus aureus* (MRSA) bacteremia (PB) outcomes related phenotypes. Relative expression of *psm*α1-4 and *psm*β1,2 (A); Neutrophils (PMN) lysis activity (B, left side) and survival to PMN exposure (B, right side); and susceptibilities to human neutrophil peptide 1 (hNP-1) (C) in clinical PB (underlined) vs resolving MRSA bacteremia strains. Data are representative of 3 independent experiments. \**P* < .05, \*\**P* < .01, \*\*\**P* < .001, \*\*\*\**P* < .0001 vs their respective PB strain by Student *t* test. Error bars represent standard deviations.

[14], thereby directly linking purine biosynthesis and (p)ppGpp in clinical PB isolates. Consistent with our hypothesis, the present investigation demonstrated that PB clinical strains (vs genetically matched RB clinical strains) exhibit significantly higher (p)ppGpp production and corresponding higher GDP/GTP levels. In parallel, mutants defective in purine synthesis (ie, *purF* mutant) exhibited lower (p)ppGpp level vs its parent and *purF*-complemented strain.

It has been reported that the stringent response positively regulates the expression of cytotoxic PSMs, especially the PSMα [29]. In turn, *S. aureus* utilizes these PSMs to modulate PMN killing by lysing these host immune cells [29, 41]. Notably, the transcription of *psm* is positively regulated by AgrA, the response regulator in the quorum-sensing *agr* system [29] and inhibited by *agr*-specific inhibitors in MRSA strain LAC\* [43]. Of great interest, our previous studies showed significantly earlier and higher *agrA* expression as a signature event in PB but not RB clinical isolates [4, 17]. In the current study, the data also revealed significantly increased (p)ppGpp production, accompanied by higher *psm*α1-4 and *psm*β1,2 expression in PB vs RB clinical strains. These themes were confirmed in a genetically defined strain set, JE2 parental and its isogenic *purF* and *relP* mutants. These findings are consistent with the results of Geiger et al, who demonstrated marked declines in *psm*α and *psm*β

expression in 2 (p)ppGpp-defective *S. aureus rel* mutants [29]. Thus, these results add credence to the plausibility that the accumulation of (p)ppGpp can lead to elevated *psm* transcription.

PSMs have an extraordinary ability to lyse and alter the functionality of many eukaryotic cell types including endothelium, erythrocytes, and most importantly for innate host defense, PMNs [41]. We found here that higher *psm* expression in PB vs RB strains correlated with greater PMN lysis and enhanced survival in PMN and upon exposure to PMN defensin hNP-1. In support of our data, Yang et al recently reported that a chromosomal mutation of *purB* (an adenylosuccinate lyase of purine biosynthesis) in JE2 background significantly attenuated neutrophil lysis and reduced virulence in a zebrafish embryo infection model [44]. Collectively, these results further validate a unique interconnection between purine biosynthesis and survival in PMN among a cadre of connected events in PB vs RB strains—purine biosynthesis, (p)ppGpp production, *psm* expression, and PMN killing/lysis—which represent a novel and coordinated mechanism promoting PB outcomes in MRSA endovascular infections.

Given the recent perspective that MRSA persistence promotes the evolution of antibiotic resistance [45], this important finding further underscores an urgent need to investigate the specific mechanism(s) of persistence. In the current study, VAN

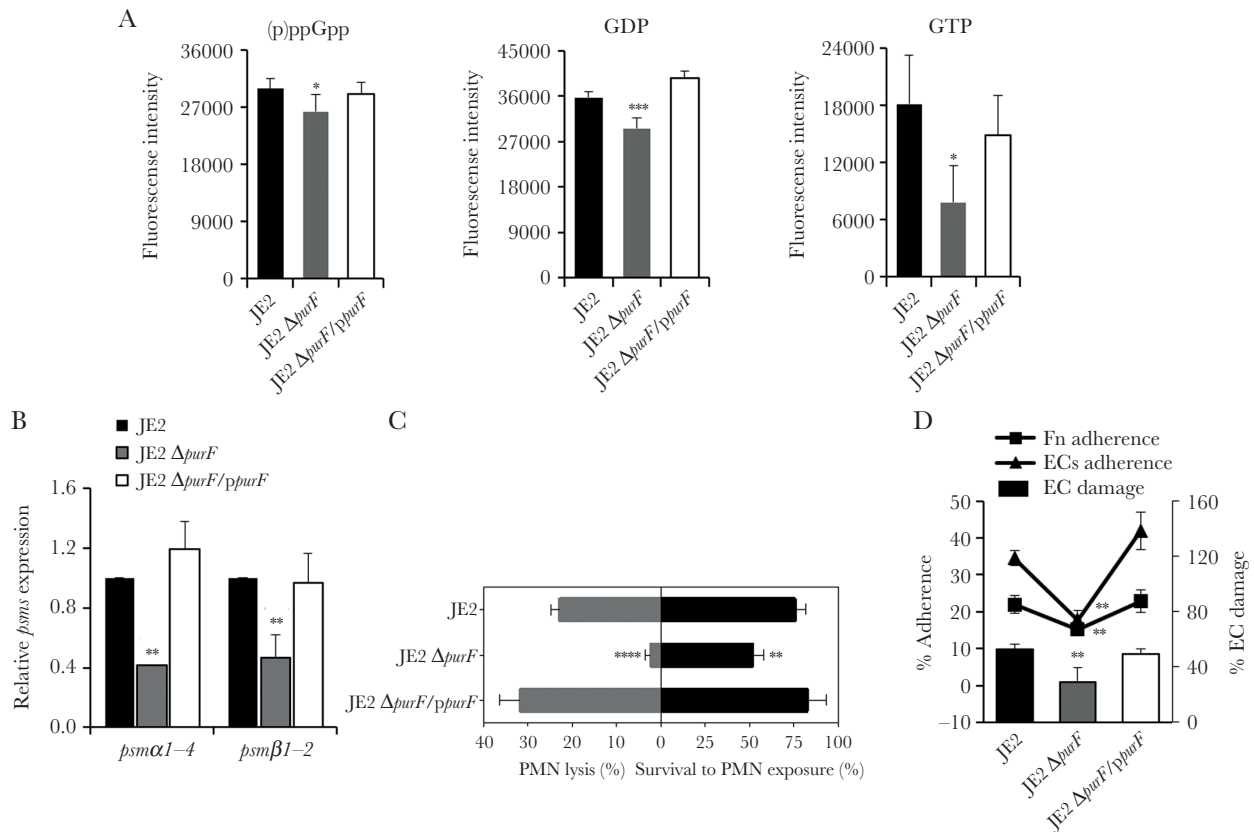


**Figure 4.** Interaction of the purine biosynthesis and stringent response. Levels of (p)ppGpp, GDP, and GTP (A); relative expression of *psm* $\alpha$ 1-4 and *psm* $\beta$ 1,2 (B); Neutrophils (PMN) lysis activity (C, left side) and survival to PMN exposure (C, right side); and fibronectin (Fn) and endothelial cell (EC) adherence and EC damage (D) in JE2 parental, its isogenic *purF* mutant, and *purF*-complemented strains. Data are representative of 3 independent experiments. \* $P < .05$ , \*\* $P < .01$ , \*\*\* $P < .001$ , \*\*\*\* $P < .0001$  vs JE2 parental and *purF*-complemented strains by Student *t* test. Error bars represent standard deviations.

showed significantly greater staphylocidal activity against a *relP* mutant variant as compared to its parental JE2 strain in vitro. These data are in accordance with Geiger et al showing that a *relP* mutant in HG001 was more susceptible to VAN-mediated killing than its parental strain [10]. Similarly, the reduced VAN resistance was also reported in *relA* and/or *relQ* mutants in *Enterococcus faecium* and *Enterococcus faecalis* strain backgrounds [46, 47]. The linkage of the stringent response to sensitivity of cell-wall active agent presumably may be due to changes in cell wall biosynthesis and/or cell wall turnover process [10]. Therefore, as purine biosynthesis positively regulates the stringent response [(p)ppGpp], the resultant increase in (p)ppGpp accumulation in PB vs RB strains appears to confer survival advantages to antibiotic challenges and immune subversion.

Most importantly, the in vitro genotypic and phenotypic findings as detailed above were translatable into significant differences in VAN treatment outcomes in the experimental IE model. For instance, animals infected with the *relP* mutant were significantly more susceptible to VAN treatment as compared to animals infected with the JE2 parental strain. Based on corroborating results generated in the current study, the PSM-related phenotypes may contribute to this in

vivo outcome through at least 2 mechanisms (Figure 1). (1) As part of the first-line innate host defense, PMNs phagocytose bacteria followed by killing via oxidative burst [48]; in response, PB strains secrete higher PSMs, inducing greater PMN lysis [29, 41]. (2) Host defense peptides (eg, hNP-1) produced from PMN granules generally provide rapid and efficient killing of invading intracellular pathogens [48]; as part of the stringent response pathway, PB strains becomes more resistant to hNP-1, thus favoring *S. aureus* survival during the initial bacteremic stage of endovascular infection [3, 38]. We previously demonstrated that higher in vitro EC damage positively correlated with poor VAN responsiveness in the same IE model due to MRSA [38, 42]. In the current study, the *purF* and *relP* mutants also showed significantly less Fn and EC adherence, and EC damage vs the isogenic parental strain, which might contribute to the hypersusceptibility to VAN treatment outcome in the IE model. In agreement with our findings, Goncheva et al recently reported that mutation of *purR*, a transcriptional repressor of purine biosynthesis, enhanced Fn adherence, and virulence in a murine bacteremia model of *S. aureus* [49]. Last, the role of the purine biosynthesis pathway and the stringent response in altering



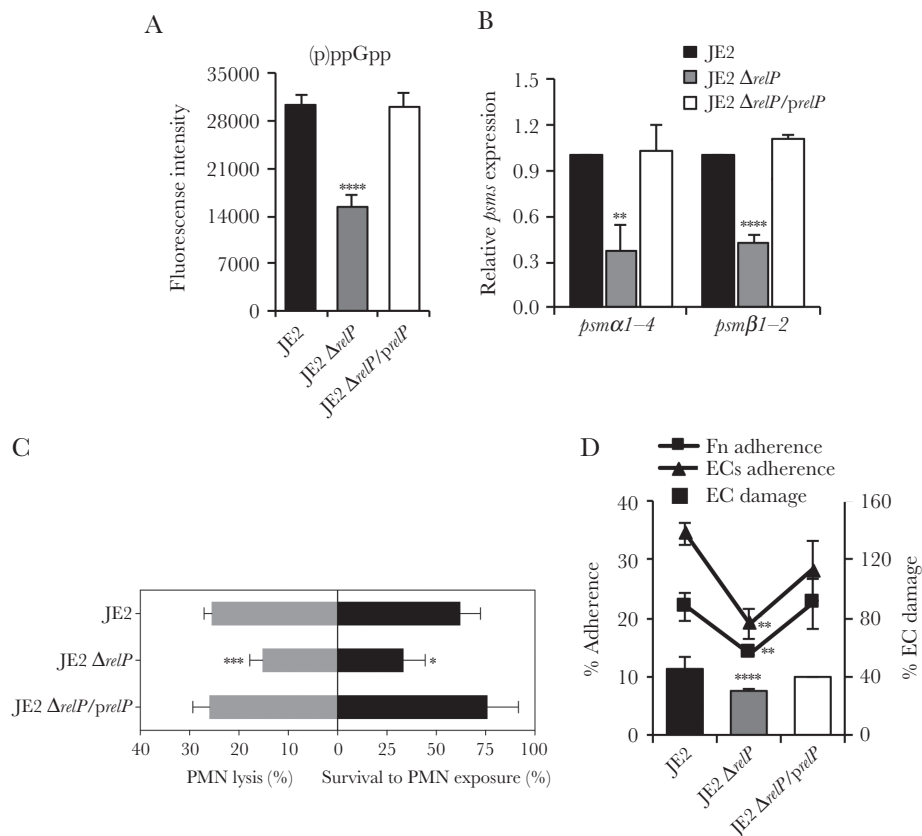


**Figure 5.** (p)ppGpp mediates *psms* expression and its impacts on persistent methicillin-resistant *Staphylococcus aureus* bacteremia (PB) outcome-related phenotypes. (p) ppGpp levels (A), relative expression of *psm* $\alpha 1-4$  and *psm* $\beta 1,2$  (B), Neutrophils (PMN) lysis activity (C, left side) and survival to PMN exposure (C, right side); and fibronectin (Fn) and endothelial cell (EC) adherence and EC damage (D) in JE2 parental, its isogenic *relP* mutant, and *relP*-complemented strains. Data are representative of 3 independent experiments. \* $P < .05$ , \*\* $P < .01$ , \*\*\* $P < .001$ , \*\*\*\* $P < .0001$  vs JE2 parental and *relP*-complemented strains by Student *t* test. Error bars represent standard deviations.

the susceptibility of VAN likely contribute to the treatment outcomes of PB MRSA infections [10, 16].

We recognize some limitations of our current study. Most importantly, in clinical settings, the phenotype of PB in patients is likely to represent a complex interaction between host and pathogen, and thus it is multifactorial. In some cases, patients

with PB may have longer duration of fever [50], while in other PB patients, all signs of sepsis and leukocytosis have resolved, especially in patients who have bacteremia for more than a week or so. Thus, it is likely that our current model system reflects some, but not all of the pathways to MRSA persistence. Taken together, persistent MRSA endovascular infection is

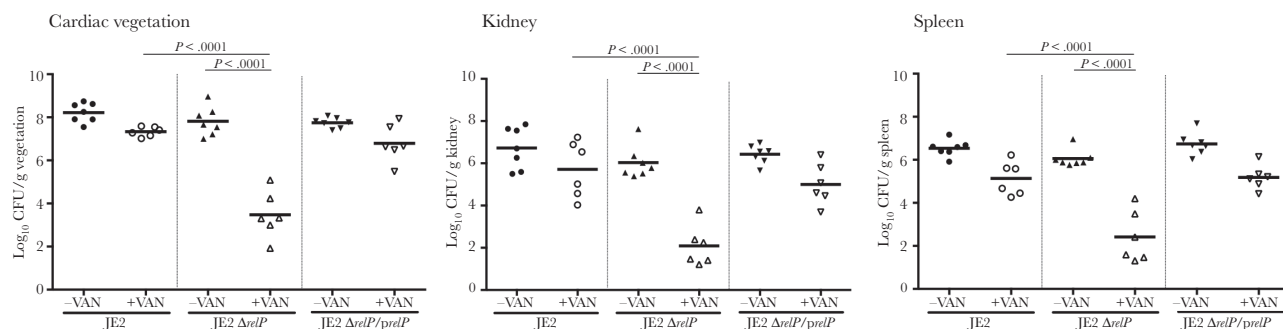


**Figure 6.** The stringent response had a significant impact on the efficacy of vancomycin (VAN) in a rabbit infective endocarditis (IE) model. Densities of methicillin-resistant *Staphylococcus aureus* (MRSA) in target tissues in the IE model due to  $10^5$  colony-forming unit (CFU) challenges of JE2 parental and its isogenic *relP*-mutant or -complemented strains with/without VAN treatment. Each dot represents 1 animal. Horizontal black bars indicate means of MRSA densities. One-way analysis of variance with Tukey multiple comparisons test (no adjustment) was used to analyze the tissue MRSA counts between different groups.

complicated, and no single system is likely to fully recapitulate the complexity of clinical PB phenotype.

In summary, the current findings support the existence of a previously unrecognized adaptive mechanism intersecting purine biosynthesis and the stringent response in persistent endovascular infections caused by MRSA strains, and provide valuable insights into how MRSA adaptively utilizes purine biosynthesis and the stringent response to evade antibiotic action and subvert immune responses to cause PB outcomes.

## Notes

**Financial support.** This work was supported by the National Institutes of Health (grant numbers R01 AI139244 to Y. Q. X; R01 AI130056 to A. S. B; and U01 AI124319 to M. R. Y).

**Potential conflicts of interest.** M. R. Y. is a founder of NovaDigm Therapeutics, Inc. In addition, M. R. Y. has the following patents issued: “Antimicrobial Kinocidins and Methods”; “Peptides and Methods Inducing PCD”; “Antimicrobial Metapeptides”; “Context-Activated Protides”; and “Anti-Infective Phenyl-OH Benzoates.” All other authors report no potential conflicts of interest.

All authors have submitted the ICMJE Form for Disclosure of Potential Conflicts of Interest. Conflicts that the editors consider relevant to the content of the manuscript have been disclosed.

## References

1. Fowler VG Jr, Miro JM, Hoen B, et al; ICE Investigators. *Staphylococcus aureus* endocarditis: a consequence of medical progress. *JAMA* **2005**; 293:3012–21.
2. Fowler VG Jr, Sakoulas G, McIntyre LM, et al. Persistent bacteremia due to methicillin-resistant *Staphylococcus aureus* infection is associated with *agr* dysfunction and low-level in vitro resistance to thrombin-induced platelet microbicidal protein. *J Infect Dis* **2004**; 190:1140–9.
3. Xiong YQ, Fowler VG, Yeaman MR, Perdreau-Remington F, Kreiswirth BN, Bayer AS. Phenotypic and genotypic characteristics of persistent methicillin-resistant *Staphylococcus aureus* bacteremia in vitro and in an experimental endocarditis model. *J Infect Dis* **2009**; 199:201–8.
4. Seidl K, Chen L, Bayer AS, Hady WA, Kreiswirth BN, Xiong YQ. Relationship of *agr* expression and function with virulence and vancomycin treatment outcomes in experimental endocarditis due to methicillin-resistant *Staphylococcus aureus*. *Antimicrob Agents Chemother* **2011**; 55:5631–9.
5. Gaca AO, Colomer-Winter C, Lemos JA. Many means to a common end: the intricacies of (p)ppGpp metabolism and its control of bacterial homeostasis. *J Bacteriol* **2015**; 197:1146–56.
6. Hauryliuk V, Atkinson GC, Murakami KS, Tenson T, Gerdes K. Recent functional insights into the role of (p)ppGpp in bacterial physiology. *Nat Rev Microbiol* **2015**; 13:298–309.
7. Liu K, Bittner AN, Wang JD. Diversity in (p)ppGpp metabolism and effectors. *Curr Opin Microbiol* **2015**; 24:72–9.
8. Steinchen W, Bange G. The magic dance of the alarmones (p)ppGpp. *Mol Microbiol* **2016**; 101:531–44.
9. Geiger T, Goerke C, Fritz M, et al. Role of the (p)ppGpp synthase RSH, a RelA/SpoT homolog, in stringent response and virulence of *Staphylococcus aureus*. *Infect Immun* **2010**; 78:1873–83.
10. Geiger T, Kästle B, Gratani FL, Goerke C, Wolz C. Two small (p)ppGpp synthases in *Staphylococcus aureus* mediate tolerance against cell envelope stress conditions. *J Bacteriol* **2014**; 196:894–902.
11. Magnusson LU, Farewell A, Nyström T. ppGpp: a global regulator in *Escherichia coli*. *Trends Microbiol* **2005**; 13:236–42.
12. Christopherson RL, Lyons SD, Wilson PK. Inhibitors of de novo nucleotide biosynthesis as drugs. *Acc Chem Res* **2002**; 35:961–71.
13. Haseltine WA, Block R, Gilbert W, Weber K. MSI and MSII made on ribosome in idling step of protein synthesis. *Nature* **1972**; 238:381–4.
14. Kriel A, Bittner AN, Kim SH, et al. Direct regulation of GTP homeostasis by (p)ppGpp: a critical component of viability and stress resistance. *Mol Cell* **2012**; 48:231–41.
15. Wang B, Dai P, Ding D, et al. Affinity-based capture and identification of protein effectors of the growth regulator ppGpp. *Nat Chem Biol* **2019**; 15:141–50.
16. Li L, Abdelhady W, Donegan NP, et al. Role of purine biosynthesis in persistent methicillin-resistant *Staphylococcus aureus* infection. *J Infect Dis* **2018**; 218:1367–77.
17. Abdelhady W, Chen L, Bayer AS, et al. Early *agr* activation correlates with vancomycin treatment failure in multi-clonotype MRSA endovascular infections. *J Antimicrob Chemother* **2015**; 70:1443–52.
18. Abdelhady W, Bayer AS, Seidl K, et al. Reduced vancomycin susceptibility in an in vitro catheter-related biofilm model correlates with poor therapeutic outcomes in experimental endocarditis due to methicillin-resistant *Staphylococcus aureus*. *Antimicrob Agents Chemother* **2013**; 57:1447–54.
19. Spentzas T, Kudumula R, Acuna C, et al. Role of bacterial components in macrophage activation by the LAC and MW2 strains of community-associated, methicillin-resistant *Staphylococcus aureus*. *Cell Immunol* **2011**; 269:46–53.
20. Manna AC, Ingavale SS, Maloney M, van Wamel W, Cheung AL. Identification of sarV (SA2062), a new transcriptional regulator, is repressed by SarA and MgrA (SA0641) and involved in the regulation of autolysis in *Staphylococcus aureus*. *J Bacteriol* **2004**; 186:5267–80.

21. Rhee HW, Lee CR, Cho SH, et al. Selective fluorescent chemosensor for the bacterial alarmone (p)ppGpp. *J Am Chem Soc* **2008**; 130:784–5.
22. Gao W, Chua K, Davies JK, et al. Two novel point mutations in clinical *Staphylococcus aureus* reduce linezolid susceptibility and switch on the stringent response to promote persistent infection. *PLoS Pathog* **2010**; 6:e1000944.
23. Corrigan RM, Bellows LE, Wood A, Gründling A. ppGpp negatively impacts ribosome assembly affecting growth and antimicrobial tolerance in gram-positive bacteria. *Proc Natl Acad Sci U S A* **2016**; 113:E1710–9.
24. Verhelst J, Spitaels J, Nürnberger C, et al. Functional comparison of Mx1 from two different mouse species reveals the involvement of loop L4 in the antiviral activity against influenza A viruses. *J Virol* **2015**; 89:10879–90.
25. Mempin R, Tran H, Chen C, Gong H, Kim Ho K, Lu S. Release of extracellular ATP by bacteria during growth. *BMC Microbiol* **2013**; 13:301.
26. McElroy WD, DeLuca MA. Firefly and bacterial luminescence: basic science and applications. *J Appl Biochem* **1983**; 5:197–209.
27. Mondal S, Hsiao K, Goueli SA. A Homogenous bioluminescent system for measuring GTPase, GTPase activating protein, and guanine nucleotide exchange factor activities. *Assay Drug Dev Technol* **2015**; 13:444–55.
28. Li L, Cheung A, Bayer AS, et al. The global regulon *sarA* regulates  $\beta$ -Lactam antibiotic resistance in methicillin-resistant *Staphylococcus aureus* in vitro and in endovascular infections. *J Infect Dis* **2016**; 214:1421–9.
29. Geiger T, Francois P, Liebeck M, et al. The stringent response of *Staphylococcus aureus* and its impact on survival after phagocytosis through the induction of intracellular PSMs expression. *PLoS Pathog* **2012**; 8:e1003016.
30. Kraus D, Herbert S, Kristian SA, et al. The GraRS regulatory system controls *Staphylococcus aureus* susceptibility to antimicrobial host defenses. *BMC Microbiol* **2008**; 8:85.
31. Katzenmeyer KN, Szott LM, Bryers JD. Artificial opsonin enhances bacterial phagocytosis, oxidative burst and chemokine production by human neutrophils. *Pathog Dis* **2017**; 75. doi:10.1093/femspd/ftx075.
32. Alazami AM, Patel N, Shamseldin HE, et al. Accelerating novel candidate gene discovery in neurogenetic disorders via whole-exome sequencing of prescreened multiplex consanguineous families. *Cell Rep* **2015**; 10:148–61.
33. Xiong YQ, Mukhopadhyay K, Yeaman MR, Adler-Moore J, Bayer AS. Functional interrelationships between cell membrane and cell wall in antimicrobial peptide-mediated killing of *Staphylococcus aureus*. *Antimicrob Agents Chemother* **2005**; 49:3114–21.
34. Chaili S, Cheung AL, Bayer AS, et al. The GraS sensor in *Staphylococcus aureus* mediates resistance to host defense peptides differing in mechanisms of action. *Infect Immun* **2016**; 84:459–66.
35. Xiong YQ, Bayer AS, Yeaman MR, Van Wamel W, Manna AC, Cheung AL. Impacts of *sarA* and *agr* in *Staphylococcus aureus* strain Newman on fibronectin-binding protein A gene expression and fibronectin adherence capacity in vitro and in experimental infective endocarditis. *Infect Immun* **2004**; 72:1832–6.
36. Ades EW, Candal FJ, Swerlick RA, et al. HMEC-1: establishment of an immortalized human microvascular endothelial cell line. *J Invest Dermatol* **1992**; 99:683–90.
37. Zell C, Resch M, Rosenstein R, Albrecht T, Hertel C, Götz F. Characterization of toxin production of coagulase-negative staphylococci isolated from food and starter cultures. *Int J Food Microbiol* **2008**; 127:246–51.
38. Seidl K, Bayer AS, Fowler VG Jr, et al. Combinatorial phenotypic signatures distinguish persistent from resolving methicillin-resistant *Staphylococcus aureus* bacteremia isolates. *Antimicrob Agents Chemother* **2011**; 55:575–82.
39. Seidl K, Zinkernagel AS. The MTT assay is a rapid and reliable quantitative method to assess *Staphylococcus aureus* induced endothelial cell damage. *J Microbiol Methods* **2013**; 92:307–9.
40. Abdelhady W, Bayer AS, Seidl K, et al. Impact of vancomycin on *sarA*-mediated biofilm formation: role in persistent endovascular infections due to methicillin-resistant *Staphylococcus aureus*. *J Infect Dis* **2014**; 209:1231–40.
41. Wang R, Braughton KR, Kretschmer D, et al. Identification of novel cytolytic peptides as key virulence determinants for community-associated MRSA. *Nat Med* **2007**; 13:1510–4.
42. Seidl K, Bayer AS, McKinnell JA, Ellison S, Filler SG, Xiong YQ. In vitro endothelial cell damage is positively correlated with enhanced virulence and poor vancomycin responsiveness in experimental endocarditis due to methicillin-resistant *Staphylococcus aureus*. *Cell Microbiol* **2011**; 13:1530–41.
43. Zhou Y, Niu C, Ma B, et al. Inhibiting PSM $\alpha$ -induced neutrophil necroptosis protects mice with MRSA pneumonia by blocking the *agr* system. *Cell Death Dis* **2018**; 9:362.
44. Yang D, Ho YX, Cowell LM, Jilani I, Foster SJ, Prince LR. A genome-wide screen identifies factors involved in *S. aureus*-induced human neutrophil cell death and pathogenesis. *Front Immunol* **2019**; 10:45.
45. Liu J, Gefen O, Ronin I, Bar-Meir M, Balaban NQ. Effect of tolerance on the evolution of antibiotic resistance under drug combinations. *Science* **2020**; 367:200–4.
46. Honsa ES, Cooper VS, Mhaisien MN, et al. RelA mutant *Enterococcus faecium* with multiantibiotic tolerance arising in an immunocompromised host. *MBio* **2017**; 8. doi:10.1128/mBio.02124-16.
47. Abranches J, Martinez AR, Kajfasz JK, Chávez V, Garsin DA, Lemos JA. The molecular alarmone (p)ppGpp mediates

- stress responses, vancomycin tolerance, and virulence in *Enterococcus faecalis*. *J Bacteriol* **2009**; 191:2248–56.
48. Nathan C. Neutrophils and immunity: challenges and opportunities. *Nat Rev Immunol* **2006**; 6:173–82.
49. Goncheva MI, Flannagan RS, Sterling BE, et al. Stress-induced inactivation of the *Staphylococcus aureus* purine biosynthesis repressor leads to hypervirulence. *Nat Commun* **2019**; 10:775.
50. Hawkins C, Huang J, Jin N, Noskin GA, Zembower TR, Bolon M. Persistent *Staphylococcus aureus* bacteremia: an analysis of risk factors and outcomes. *Arch Intern Med* **2007**; 167:1861–7.